

## Tuning the Band Gap of Low-Band-Gap Polyselenophenes and Polythiophenes: The Effect of the Heteroatom<sup>†</sup>

Asit Patra,<sup>‡</sup> Yair H. Wijsboom,<sup>‡</sup> Gregory Leitus,<sup>§</sup> and Michael Bendikov<sup>\*,‡</sup>

<sup>‡</sup>Department of Organic Chemistry and <sup>§</sup>Chemical Research Support Unit,  
Weizmann Institute of Science, Rehovot 76100, Israel

Received August 19, 2010. Revised Manuscript Received December 16, 2010

A series of new low-band-gap thieno- or selenolo-fused polyselenophenes (**P5** and **P6**) and selenolo-fused polythiophene (**P4**) (as well as previously reported thieno-fused polythiophene, **P3**) was prepared systematically by electropolymerization (**P4–P6**) and by solid-state polymerization (**P3**, **P5** and **P6**). The 2,5-dibrominated monomers (**3Br<sub>2</sub>**, **5Br<sub>2</sub>**, and **6Br<sub>2</sub>**) undergo solid-state polymerization under slight heating and produce insoluble **P3**, **P5**, and **P6** as black conducting powders. The spectroelectrochemically measured optical band gaps of **P4–P6** films are 0.96, 0.72, and 0.76 eV, respectively. DFT calculations performed on **P3–P6** provide excellent estimations of the experimental band gaps of these polymers. The band gap of the polyselenophenes (**P5** and **P6**) is 0.2 eV lower than that of the corresponding polythiophenes (**P3** and **P4**). We introduced a new scheme for band gap control in conjugated polymers by replacing the sulfur atom with a selenium atom in the main and/or peripheral ring, which leads to significant and predictable changes in the band gap of the polymers. This is due to the lower aromaticity of a selenophene ring compared to a thiophene ring. Thus, we have achieved band gap control in very low band gap (~0.7–1.0 eV) polymers through the use of different combinations of selenium and sulfur atoms in the main and peripheral rings.

### Introduction

Conjugated polymers have attracted considerable interest because of their tunable electronic properties and wide range of possible applications.<sup>1</sup> Special attention has been devoted to low-band-gap conjugated polymers<sup>2</sup> originally because of their unique electronic properties and recently on account of their ability to efficiently absorb solar light and the promise they show as materials to improve photovoltaic cells.<sup>3,4</sup>

The band gap of conjugated polymers (which are build from aromatic units) depends (among other factors) on the degree of a quinoid or aromatic character of the backbone. A powerful approach to designing low-band-gap polymers is to use the donor–acceptor concept.<sup>2,5–7</sup> Another very important strategy for designing low-band-gap conducting polymers is to incorporate fused aromatic ring(s) into the monomer skeleton to enhance the quinoid character of the polymer backbone.<sup>8–10</sup> The first and classical example of the later strategy is the synthesis of poly(isothianaphthene) (PITN).<sup>8,11</sup> The aromaticity of the fused benzo or heterocyclic ring enforces a quinoid structure on the backbones, which leads to a low

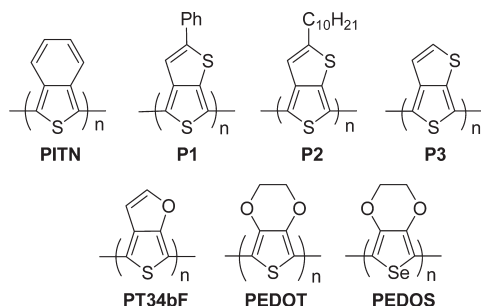
<sup>†</sup> Accepted as part of the “Special Issue on  $\pi$ -Functional Materials”.

\*Corresponding author. E-mail: michael.bendikov@weizmann.ac.il.

- (1) (a) *Handbook of Conducting Polymers*, 3rd ed.; Skotheim, T. A., Reynolds, J. R., Eds.; CRC Press: Boca Raton, FL, 2007. (b) *Handbook of Organic Conductive Molecules and Polymers*; Nalwa, H. S., Ed.; John Wiley & Sons: New York, 1997.
- (2) Rasmussen, C. S.; Pomerantz, M. In *Handbook of Conducting Polymers: Theory, Synthesis, Properties and Characterization*, 3rd ed.; Skotheim, T. A., Reynolds, J. R., Eds.; CRC Press: Boca Raton, FL, 2007, Chapter 12, pp 12.1–12.42.
- (3) (a) Mozer, A. J.; Sariciftci, N. S. In *Handbook of Conducting Polymers: Processing and Applications*, 3rd ed.; Skotheim, T. A., Reynolds, J. R., Eds.; CRC Press: Boca Raton, FL, 2007, Chapter 10, pp 10.1–10.37. (b) Gevorgyan, S. A.; Krebs, F. C. In *Handbook of Thiophene-Based Materials*; Perepichka, I. F., Perepichka, D. F., Eds.; Wiley-VCH: Chichester, U.K., 2009; Chapter 18, pp 673–694. (c) Mishra, A.; Ma, C. Q.; Bäuerle, P. *Chem. Rev.* **2009**, *109*, 1141–1276. (d) Cheng, Y. J.; Yang, S. H.; Hsu, C. S. *Chem. Rev.* **2009**, *109*, 5868–5923.
- (4) (a) Zoombelt, A. P.; Gilot, J.; Wienk, M. M.; Janssen, R. A. J. *Chem. Mater.* **2009**, *21*, 1663–1669. (b) Zoombelt, A. P.; Fonrodona, M.; Wienk, M. M.; Sieval, A. B.; Hummelen, J. C.; Janssen, R. A. J. *Org. Lett.* **2009**, *11*, 903–906. (c) Chen, H. Y.; Hou, J. H.; Zhang, S. Q.; Liang, Y. Y.; Yang, G. W.; Yang, Y.; Yu, L. P.; Wu, Y.; Li, G. *Nat. Photonics* **2009**, *3*, 649–653.

- (5) Ajayaghosh, A. *Chem. Soc. Rev.* **2003**, *32*, 181–191.
- (6) Salzner, U. *J. Phys. Chem. B* **2002**, *106*, 9214–9220.
- (7) (a) Xia, Y.; Wang, L.; Deng, X.; Li, D.; Zhu, X.; Cao, Y. *Appl. Phys. Lett.* **2006**, *89*, 081106/1–081106/3. (b) Steckler, T. T.; Abboud, K. A.; Craps, M.; Rinzler, A. G.; Reynolds, J. R. *Chem. Commun.* **2007**, 4904–4906. (c) Sonmez, G.; Meng, H.; Wudl, F. *Chem. Mater.* **2003**, *15*, 4923–4929. (d) Zhu, Y.; Champion, R. D.; Jenekhe, S. A. *Macromolecules* **2006**, *39*, 8712–8719.
- (8) Wudl, F.; Kobayashi, M.; Heeger, A. J. *J. Org. Chem.* **1984**, *49*, 3382.
- (9) Sotzing, A. G.; Seshadri, V.; Waller, J. F. P. In *Handbook of Conducting Polymers: Theory, Synthesis, Properties and Characterization*, 3rd ed.; Skotheim, T. A., Reynolds, J. R., Eds.; CRC Press: Boca Raton, FL, 2007; Chapter 11, pp 11.1–11.18.
- (10) Kiebooms, R.; Hoogmartens, I.; Adriaenssens, P.; Vanderzande, D.; Gelan, J. *Macromolecules* **1995**, *28*, 4961–4969.
- (11) (a) Kobayashi, M.; Colaneri, N.; Boysel, M.; Wudl, F.; Heeger, A. J. *J. Chem. Phys.* **1985**, *82*, 5717. (b) Colaneri, N.; Kobayashi, M.; Heeger, A. J.; Wudl, F. *Synth. Met.* **1986**, *14*, 45.
- (12) Viruela, P. M.; Viruela, R.; Ortí, E.; Brédas, J. L. *J. Am. Chem. Soc.* **1997**, *119*, 1360–1369.

band gap and a greater tendency to maintain planarity. However, PITN is not planar<sup>12,13</sup> because of repulsion between the sulfur atom and hydrogen atom on the phenyl ring and, consequently, its band gap is above 1.0 eV. Another example is thieno-fused thiophenes,<sup>14</sup> such as poly(2-phenylthieno[3,4-*b*]thiophene) (**P1**)<sup>15</sup> and poly(2-decylthieno[3,4-*b*]thiophene) (**P2**),<sup>16</sup> which are expected to be planar. Using this strategy, Sotzing and co-workers reported two unsubstituted thieno- and furan-fused polythiophene-based polymers, poly(thieno[3,4-*b*]thiophene) (PT34bT; **P3**)<sup>17,18</sup> and poly(thieno[3,4-*b*]furan) (PT34bF)<sup>19</sup> having low band gaps of 0.85 and 1.03 eV, respectively. After this manuscript was submitted, we came across the article describing a new synthetic route for monomers thieno[3,4-*b*]thiophene (**3**), its alkyl derivatives, selenolo[3,4-*b*]thiophene (**5**) and thieno[3,4-*b*]furan in multistep synthesis,<sup>19c</sup> which is different from the one used in our study. In the last year, the thieno[3,4-*b*]thiophene (**3**) unit has attracted significant attention as a building block for the construction of low-band-gap polymers for solar-cell applications and the highest efficiency for an organic solar cell, 6.77%, was achieved using a substituted thieno[3,4-*b*]thiophene building block.<sup>4c,20</sup>



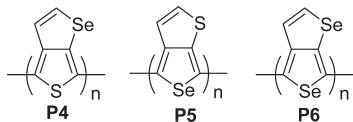
Thiophene-based conducting polymers having a fused heterocyclic ring (e.g., poly(3,4-ethylenedioxythiophene),

PEDOT,<sup>21</sup> and its derivatives) are well-studied and are finding commercial applications. Recently, we reported<sup>22,23</sup> poly(3,4-ethylenedioxythiophene) (PEDOS), a selenium analogue of PEDOT, which shows a low band gap, very high stability in the oxidized state, and a well-defined spectroelectrochemistry. PEDOS ( $E_g = 1.4$  eV) has a band gap 0.2 eV lower than that of PEDOT ( $E_g = 1.6$  eV).<sup>22</sup> PEDOS derivatives also compare favorably with PEDOT derivatives in some cases.<sup>24,25</sup> Other polyselenophenes have been reported recently.<sup>23,26,27</sup> As a class, polyselenophenes are expected to have advantages over polythiophenes. For example, interchain charge transfer should be facilitated by intermolecular Se...Se contacts. Furthermore, both experimental<sup>22,25</sup> and theoretical studies<sup>28,29</sup> indicate that polyselenophenes should have a lower band gap, a more quinoid character, and importantly, should be more difficult to twist<sup>25,29</sup> than polythiophenes. Consequently, polyselenophenes are attractive candidates for the synthesis of low-band-gap conjugated polymers. Selenophene also has a lower aromaticity than thiophene,<sup>30</sup> so a fused selenophene ring should enforce a less quinoid structure on the polymer backbone. We propose that these properties of polyselenophenes and the fused selenophene ring can also be used for band gap control purposes in conjugated polymers.

Inspired by the high stability, low band gap, and promising properties of PEDOS<sup>22</sup> and its derivatives,<sup>23–25</sup> we decided to extend our study to the selenium analogues of known **P3**<sup>17</sup> in order to achieve lowering of the band gap and a more effective band gap control in conjugated polymers. Here, we introduce a new method for band gap control in very low band gap polymers. Our method takes advantage of the different aromaticity of the selenophene ring versus the thiophene ring to enable band gap tuning in the range of 0.7–1.0 eV. We also present an efficient synthetic method, characterization, and comparative DFT calculations for new low-band-gap polymers, poly(selenolo[2,3-*c*]thiophene) (**P4**), poly(selenolo[3,4-*b*]thiophene) (**P5**), and poly(selenolo[3,4-*b*]selenophene)

- (13) Our calculations of the minimal geometry of PITN (at PBC/B3LYP/6-31G(d)) and of the geometry of long (up to 15-mer) INT oligomers (at B3LYP/6-31G(d)) lead to nonplanar (twisted or bended) structures.
- (14) (a) Skabara, J. P. In *Handbook of Thiophene-Based Materials*; Perepichka, I. F., Perepichka, D. F., Eds.; Wiley-VCH: Chichester, U.K., 2009; Chapter 3, pp 219–254. (b) Litvinov, V. P. *Adv. Heterocycl. Chem.* **2006**, 90, 125–203.
- (15) Neef, C. J.; Brotherston, I. D.; Ferraris, J. P. *Chem. Mater.* **1999**, 11, 1957–1958.
- (16) (a) Pomerantz, M.; Gu, X.; Zhang, S. X. *Macromolecules* **2001**, 34, 1817–1822. (b) Pomerantz, M.; Gu, X. *Synth. Met.* **1997**, 84, 243–244.
- (17) (a) Lee, K.; Sotzing, G. A. *Macromolecules* **2001**, 34, 5746–5747. (b) Sotzing, G. A.; Lee, K. *Macromolecules* **2002**, 35, 7281–7286.
- (18) (a) Lee, B.; Yavuz, M. S.; Sotzing, G. A. *Macromolecules* **2006**, 39, 3118–3124. (b) Lee, B.; Seshadri, V.; Palko, H.; Sotzing, G. A. *Adv. Mater.* **2005**, 17, 1792–1795.
- (19) (a) Kumar, A.; Buyukmumcu, Z.; Sotzing, G. A. *Macromolecules* **2006**, 39, 2723–2725. (b) Kumar, A.; Bokria, J. G.; Buyukmumcu, Z.; Dey, T.; Sotzing, G. A. *Macromolecules* **2008**, 41, 7098–7108. (c) Dey, T.; Navarathne, D.; Invernale, M. A.; Berghorn, I. D.; Sotzing, G. A. *Tetrahedron Lett.* **2010**, 51, 2089–2091.
- (20) (a) Hou, J.; Chen, H. Y.; Zhang, S.; Chen, R. I.; Yang, Y.; Wu, Y.; Li, G. *J. Am. Chem. Soc.* **2009**, 131, 15586–15587. (b) Liang, Y.; Feng, D.; Wu, Y.; Tsai, S.-T.; Li, G.; Ray, C.; Yu, L. *J. Am. Chem. Soc.* **2009**, 131, 7792–7799.
- (21) (a) Groenendaal, L. B.; Jonas, F.; Freitag, D.; Pielartzik, H.; Reynolds, J. R. *Adv. Mater.* **2000**, 12, 481–494. (b) Groenendaal, L. B.; Zotti, G.; Aubert, P.-H.; Waybright, S. M.; Reynolds, J. R. *Adv. Mater.* **2003**, 15, 855–879.
- (22) Patra, A.; Wijsboom, Y. H.; Zade, S. S.; Li, M.; Sheynin, Y.; Leitus, G.; Bendikov, M. *J. Am. Chem. Soc.* **2008**, 130, 6734–6736.
- (23) Patra, A.; Bendikov, M. *J. Mater. Chem.* **2010**, 20, 422–433.
- (24) (a) Li, M.; Patra, A.; Sheynin, Y.; Bendikov, M. *Adv. Mater.* **2009**, 21, 1707–1711. (b) Li, M.; Sheynin, Y.; Patra, A.; Bendikov, M. *Chem. Mater.* **2009**, 21, 2482–2488.
- (25) Wijsboom, Y. H.; Patra, A.; Zade, S. S.; Li, M.; Sheynin, Y.; Shimon, L. J. W.; Bendikov, M. *Angew. Chem., Int. Ed.* **2009**, 48, 5443–5447.
- (26) (a) Heeney, M.; Zhang, W.; Crouch, D. J.; Chabinyc, M. L.; Gordeyev, S.; Hamilton, R.; Higgins, S. J.; McCulloch, I.; Skabara, P. J.; Sparrowe, D.; Tierney, S. *Chem. Commun.* **2007**, 5061–5063. (b) Ballantyne, A. M.; Chen, L. C.; Nelson, J.; Bradley, D. D. C.; Astuti, Y.; Maurano, A.; Shuttle, C. G.; Durrant, J. R.; Heeney, M.; Duffy, W.; McCulloch, I. *Adv. Mater.* **2007**, 19, 4544–4547.
- (27) Das, S.; Zade, S. S. *Chem. Commun.* **2010**, 46, 1168–1170.
- (28) (a) Salzner, U.; Lagowski, J. B.; Pickup, P. G.; Poirier, R. A. *Synth. Met.* **1998**, 96, 177–189. (b) Zade, S. S.; Bendikov, M. *Org. Lett.* **2006**, 8, 5243–46. (c) Zade, S. S.; Bendikov, M. *Chem.—Eur. J.* **2008**, 14, 6734–6741.
- (29) Zade, S. S.; Zamoshchik, N.; Bendikov, M. *Chem.—Eur. J.* **2009**, 15, 8613–8624.
- (30) (a) Fringuelli, F.; Marino, G.; Taticchi, A. *J. Chem. Soc., Perkin Trans. 2* **1974**, 332–337. (b) Lumbruso, H.; Bertin, D. M. *J. Chem. Soc., Perkin Trans. 2* **1977**, 775–781. (c) Chamizo, J. A.; Morgado, J.; Sosa, P. *Organometallics* **1993**, 12, 5005–5007. (d) Chen, Z.; Wannere, C. S.; Corminboeuf, C.; Puchta, R.; Schleyer, P. v. R. *Chem. Rev.* **2005**, 105, 3842–3888.

(P6).<sup>31,32</sup> We also report synthesis of **P3**, **P5**, and **P6** via solid-state polymerization (SSP) and show that polysele-nophenes are attractive candidates for very low band gap conjugated polymers.



## Experimental Section

**General Details.** All reagents were purchased from Sigma-Aldrich in reagent grade and were used without purification unless noted. <sup>1</sup>H NMR and <sup>13</sup>C NMR spectra were recorded in CDCl<sub>3</sub> on a 250 MHz spectrometer with tetramethylsilane (TMS) as the external standard. <sup>77</sup>Se NMR spectra were recorded on a 500 MHz NMR in CDCl<sub>3</sub> with chemical shifts given with respect to SeMe<sub>2</sub> for which δ<sup>77</sup>Se = 0 ppm (selenophene was used as an external standard for which δ<sup>77</sup>Se = 605 ppm). Differential scanning calorimetry (DSC) measurements were performed on a TA Q200 DSC instrument. High-resolution mass spectra were measured on a Waters Micromass GCT Premier mass spectrometer using field desorption (FD) ionization. Diethyl ether was distilled from sodium/benzophenone under an atmosphere of dry argon. In most of the column chromatographic separations, hexane was used as eluents. Columns were prepared with silica gel (60–230 mesh).

**Electrochemistry.** All electrochemical measurements were performed using a PAR 263A potentiostat in a standard three-electrode, one compartment configuration equipped with Ag/AgCl wire, Pt wire, and Pt disk electrodes (diameter 1.6 mm) as the pseudo reference electrode, counter electrode, and working electrode, respectively. Most electrochemical experiments were performed in anhydrous acetonitrile (ACN) or anhydrous dichloromethane (DCM) and propylene carbonate (PC) with 0.1 M tetrabutylammonium perchlorate (TBAPC, Fluka) or tetrabutylammonium hexafluorophosphate (TBAPF<sub>6</sub>, Fluka) (dried under vacuum) as the supporting electrolyte. All electrochemical solutions were purged with dry N<sub>2</sub> for 15 min. Ferrocene powder (Fluka) was used to establish an electrochemical internal reference for all measurements as ferrocene/ferrocenium redox couple (Fc/Fc<sup>+</sup> = 0.37 V vs saturated calomel electrode (SCE)). Monomer concentration was ~0.01 M.

**Spectroelectrochemistry.** Spectra were taken in a UV–vis–NIR quartz optical cell (100-QX, Hellma) with a JASCO V–570 UV–vis–NIR spectrophotometer. Monomers were polymerized on an indium tin oxide (ITO) working electrode (5–15 Ω/□, Delta Technologies, Stillwater). Films were electrodeposited as follows: monomers **4** and **6** were polymerized in TBAPC/ACN

at 100 mV/s and **5** was polymerized in TBAPF<sub>6</sub>/DCM at 50 mV/s in cyclic voltammetry (CV) mode. Films were washed with dichloromethane and stored under vacuum until needed. Spectroelectrochemistry experiments were performed in 0.1 M TBAPC in PC. Under these conditions, Fc/Fc<sup>+</sup> = 0.34 V vs SCE.

**Synthesis of 2,3,4,5-Tetrabromoselenophene.** Adapted from the published procedure with modification.<sup>33</sup> Bromine (94 g) in CHCl<sub>3</sub> (60 mL) was added dropwise to a stirred solution of selenophene (15 g) in CHCl<sub>3</sub> (60 mL) and AcOH (10 mL) at 0 °C over the course of 1 h. The reaction mixture was warmed to room temperature and stirred for 12 h, and then heated to 70 °C for 5 h. Upon completion of the reaction, the mixture was allowed to cool to room temperature and transferred to a large beaker. Excess bromine was evaporated at room temperature and the resulting mixture was diluted with CHCl<sub>3</sub> (200 mL). The organic phase was successively washed with water (80 mL), dilute NaOH solution (50 mL), and brine (60 mL), and then concentrated. The crude crystalline product was further purified by column chromatography using hexane as an eluent to give a white crystalline solid (46.5 g, 91% yield). mp. 98–99 °C; <sup>13</sup>C NMR (62.5 MHz, CDCl<sub>3</sub>) δ 117.9, 112.2.

**Synthesis of 3,4-Dibromoselenophene.** *n*-BuLi (1.6 M in hexanes, 29.5 mL, 47.0 mmol) was added dropwise to a stirred solution of 2,3,4,5-tetrabromoselenophene (10 g, 22.4 mmol) in anhydrous ether (80 mL) under a nitrogen atmosphere at –78 °C over the course of 30 min, and the mixture was stirred for another 1.5 h at that temperature. Water (5 mL) was added slowly to the reaction mixture, which was then allowed to warm to room temperature. The mixture was then diluted with water (100 mL), extracted with ether (3 × 75 mL), and the combined organic phases were washed with water (50 mL), brine, dried over MgSO<sub>4</sub>, and concentrated. The resulting colorless oil was purified by column chromatography using hexane as an eluent to give 3,4-dibromoselenophene (5.3 g, 82% yield) as a colorless oil. <sup>1</sup>H NMR (250 MHz, CDCl<sub>3</sub>) δ 7.93; <sup>13</sup>C NMR (62.5 MHz, CDCl<sub>3</sub>) δ 127.4, 114.3. Selective debromination of 2,3,4,5-tetrabromoselenophene with 2 equiv. of *n*-BuLi to produce 3,4-dibromoselenophene was mentioned in ref 34, although synthetic details were not reported.

**General Procedure for Synthesis of Compounds 7 and 8.** This procedure was adapted from the published procedure for compound 7.<sup>35</sup> 3,4-Dibromothiophene or 3,4-dibromoselenophene (8 mmol) was added to a stirred solution of trimethylsilylacetylene (813 mg, 1.17 mL, 8.30 mmol), PdCl<sub>2</sub> (60 mg), and PPh<sub>3</sub> (40 mg) in diethylamine (8 mL) under an inert atmosphere. To this stirred mixture was added CuI (200 mg) and the mixture was then warmed to 50 °C. After 5 h, the temperature of the reaction mixture increased to 75 °C and stirring was continued for an additional 2 h. After cooling to room temperature, 100 mL of water was added. The aqueous layer was extracted with ether (3 × 50 mL), and the combined organic layers were washed with brine and water. The resulting ether solution was dried over MgSO<sub>4</sub> and evaporated under a vacuum. The crude product was purified by column chromatography using hexane as an eluent on silica gel to obtain a pure product.

**3-Bromo-4-(trimethylsilyl)ethynylthiophene (7) (refs 35 and 36).** Colorless oil. <sup>1</sup>H NMR (250 MHz, CDCl<sub>3</sub>) δ 7.47 (d, *J* = 3.2 Hz, 1H), 7.22 (d, *J* = 3.2 Hz, 1H), 0.26 (s, 9H). <sup>13</sup>C NMR

- (31) After this work was completed, compounds **4**–**6** and their polymerization were disclosed in patent applications: (a) Zahn, S.; Costello, C. A.; McLaws, M. US Pat. No. 18348, 2009. (b) Zahn, S. US Pat. No. 14693, 2009. (c) Zahn, S.; Costello, C. A.; McLaws, M. EP Pat. No. 2014664, 2009. The electrochemical polymerization of monomer **4** and the optical band gap of **P4** were reported in patent applications: (d) Zahn, S. U.S. Pat. No. 140219, 2009. (e) Zahn, S. EP Pat. No. 2014665, 2009. No other polymer characterization was provided in these patent applications.
- (32) The formal names of these materials follow the rules of IUPAC nomenclature and therefore relate first to the heaviest atom (Se) regardless of if it is positioned on the backbone or a peripheral ring. By contrast, from a materials chemistry perspective, the polymers are defined by their backbones and, thus, we refer to **P4** as a polythiophene and **P5** and **P6** as polyselenophenes.

- (33) Tung, D. T.; Villinger, A.; Langer, P. *Adv. Synth. Catal.* **2008**, *350*, 2109–2117.
- (34) Ketcham, R.; Hoernfeldt, A.-B.; Gronowitz, S. *J. Org. Chem.* **1984**, *49*, 1117–1119.
- (35) Brandsma, L.; Verkruijsse, H. D. *Synth. Commun.* **1990**, *20*, 2275–2277.



(62.5 MHz,  $\text{CDCl}_3$ )  $\delta$  129.7, 124.6, 122.8, 113.9, 97.9, 97.8,  $-0.9$ . HRMS for  $\text{C}_9\text{H}_{11}\text{BrSSi}$  [ $\text{M}^+$ ]: calcd, 257.9534 and 259.9513; found, 257.9527 and 259.9507.

**3-Bromo-4-(trimethylsilyl)ethynylselenophene (8)** (ref 31). Colorless oil.  $^1\text{H}$  NMR (250 MHz,  $\text{CDCl}_3$ )  $\delta$  8.15 (d,  $J = 3.0$  Hz, 1H), 7.85 (d,  $J = 3.0$  Hz, 1H), 0.26 (s, 9H).  $^{13}\text{C}$  NMR (62.5 MHz,  $\text{CDCl}_3$ )  $\delta$  135.5, 127.1, 126.5, 114.2, 99.9, 96.9,  $-0.3$ .

**General Procedure for Synthesis of Compounds 3–6.** Adapted from the published procedure for compound 3.<sup>17b,35</sup>  $n\text{-BuLi}$  (1.6 M in hexanes, 3.28 mmol) was added dropwise to a stirred solution of compound 7 or 8 (3.28 mmol) in dry ether (40 mL) at  $-78^\circ\text{C}$  (acetone/dry ice bath) under an inert atmosphere. The resulting mixture was stirred at  $-78^\circ\text{C}$  for 1 h, after which sulfur powder or elemental selenium (1.0 equiv.) was added to it. After these additions, the solution was stirred for 1 h at  $-78^\circ\text{C}$ , and the reaction mixture was brought to  $-10^\circ\text{C}$  over a period of 1 h and further stirred for 30 min at  $-10^\circ\text{C}$  to fully dissolve the sulfur or selenium. Then the resulting reaction mixture was added to a separatory funnel containing a 100 mL ice and brine mixture held at  $0^\circ\text{C}$ . The extraction process was completed within 1 min at  $0^\circ\text{C}$ . The organic layer was washed again with ice cold water (50 mL). The resulting aqueous part was slowly heated to  $70^\circ\text{C}$  for 1 h. After cooling, the aqueous layer was extracted with ether ( $3 \times 25$  mL) and the combined organic layers were washed with brine and water. The resulting ether solution was dried over  $\text{MgSO}_4$  and evaporated under vacuum. The crude product was purified by column chromatography using hexane as an eluent on silica gel to obtain a pure product.

**Thieno[3,4-*b*]thiophene (3)** (ref 17). Colorless oil. 63% yield.  $^1\text{H}$  NMR (250 MHz,  $\text{CDCl}_3$ )  $\delta$  7.34 (d,  $J = 5.7$  Hz, 1H), 7.35 (d,  $J = 2.2$  Hz, 1H), 7.24 (dd,  $J = 2.5$  Hz, 0.7 Hz, 1H), 6.92 (dd,  $J = 5.5$  Hz, 0.7 Hz, 1H).

**Selenolo[3,4-*b*]thiophene (4)**. Colorless oil; 61% yield;  $^1\text{H}$  NMR (250 MHz,  $\text{CDCl}_3$ )  $\delta$  7.76 (d,  $J = 6.0$  Hz, 1H), 7.41 (d,  $J = 2.7$  Hz, 1H), 7.26 (dd,  $J = 2.7$  Hz, 0.7 Hz, 1H), 7.17 (dd,  $J = 6.0$  Hz, 0.7 Hz, 1H).  $^{13}\text{C}$  NMR (62.5 MHz,  $\text{CDCl}_3$ )  $\delta$  149.8, 135.7, 132.0, 120.3, 114.4, 114.2.  $^{77}\text{Se}$  NMR ( $\text{CDCl}_3$ )  $\delta = 434$  ppm. HRMS for  $\text{C}_6\text{H}_4\text{SSe}$  [ $\text{M}^+$ ]: calcd, 187.9199; found, 187.9194.

**Selenolo[2,3-*c*]thiophene (5)**. Colorless oil; 51% yield  $^1\text{H}$  NMR (250 MHz,  $\text{CDCl}_3$ )  $\delta$  8.01 (d,  $J = 2.3$  Hz, 1H), 7.89 (dd,  $J = 2.3$  Hz, 0.8 Hz, 1H), 7.43 (d,  $J = 5.8$  Hz, 1H), 6.79 (dd,  $J = 5.9$  Hz, 0.8 Hz, 1H).  $^{13}\text{C}$  NMR (62.5 MHz,  $\text{CDCl}_3$ )  $\delta$  150.2, 141.2, 132.6, 117.4, 117.2, 114.8.  $^{77}\text{Se}$  NMR ( $\text{CDCl}_3$ )  $\delta = 737$  ppm. HRMS for  $\text{C}_6\text{H}_4\text{SSe}$  [ $\text{M}^+$ ]: calcd, 187.9199; found, 187.9205.

**Selenolo[3,4-*b*]selenophene (6)**. Low melting point white solid; 57% yield;  $^1\text{H}$  NMR (250 MHz,  $\text{CDCl}_3$ )  $\delta$  8.08 (d,  $J = 2.25$  Hz, 1H), 7.90 (dd,  $J = 0.7$  Hz, 2.25 Hz, 1H), 7.84 (d,  $J = 6$  Hz, 1H), 7.04 (dd,  $J = 6$  Hz, 0.7 Hz, 1H).  $^{13}\text{C}$  NMR (125 MHz,  $\text{CDCl}_3$ )  $\delta$  152.3, 137.0, 131.5, 120.8, 119.9, 118.0.  $^{77}\text{Se}$  NMR ( $\text{CDCl}_3$ )  $\delta = 736, 434$  ppm.

**General Procedure for Bromination of 3–6 to Obtain Dibromo-Derivatives 3Br<sub>2</sub>–6Br<sub>2</sub>.** NBS (4 mmol; recrystallized from hot water) was added to a stirred solution of compounds 3–6 (2 mmol) in  $\text{CHCl}_3$  at  $0^\circ\text{C}$ . The resulting reaction mixture was continuously stirred at  $0^\circ\text{C}$  for 20 min. The reaction was followed by TLC and, upon completion of the reaction, the mixture was diluted with water (100 mL). The resulting aqueous layer was extracted with  $\text{CHCl}_3$  ( $3 \times 40$  mL). The combined organic phases were washed with water, brine, and concentrated. Purification of the crude residue by column chromatography on silica gel

(hexanes) afforded 4,6-dibromo derivatives (3Br<sub>2</sub>–6Br<sub>2</sub>). Single crystals of 3Br<sub>2</sub> and 4Br<sub>2</sub> were obtained by slow evaporation of chloroform solution with a few drops of hexane (about 5%) in a refrigerator ( $+4^\circ\text{C}$ ).

**4,6-Dibromothieno[3,4-*b*]thiophene (3Br<sub>2</sub>).** White crystalline solid. 93% yield. M.p.  $59\text{--}60^\circ\text{C}$ .  $^1\text{H}$  NMR (250 MHz,  $\text{CDCl}_3$ )  $\delta$  7.35 (d,  $J = 5.6$  Hz, 1H), 6.78 (d,  $J = 5.6$  Hz, 1H).  $^{13}\text{C}$  NMR (62.5 MHz,  $\text{CDCl}_3$ )  $\delta$  147.1, 140.3, 133.9, 117.2, 97.1, 96.4.

**4,6-Dibromoselenolo[2,3-*c*]thiophene (4Br<sub>2</sub>).** White crystalline solid. 90% yield. M.p.  $52\text{--}53^\circ\text{C}$ .  $^1\text{H}$  NMR (250 MHz,  $\text{CDCl}_3$ )  $\delta$  7.79 (d,  $J = 6$  Hz, 1H), 7.07 (d,  $J = 6$  Hz, 1H).  $^{13}\text{C}$  NMR (62.5 MHz,  $\text{CDCl}_3$ )  $\delta$  148.9, 137.6, 133.8, 120.6, 100.3, 99.4. HRMS for  $\text{C}_6\text{H}_2\text{Br}_2\text{SSe}$  [ $\text{M}^+$ ]: calcd, 343.7409; found, 343.7387.

**4,6-Dibromoselenolo[3,4-*b*]thiophene (5Br<sub>2</sub>).** White crystalline solid. 41% yield. M.p.  $72\text{--}73^\circ\text{C}$ .  $^1\text{H}$  NMR (250 MHz,  $\text{CDCl}_3$ )  $\delta$  7.43 (d,  $J = 5.6$  Hz, 1H), 6.68 (d,  $J = 5.6$  Hz, 1H).  $^{13}\text{C}$  NMR (62.5 MHz,  $\text{CDCl}_3$ )  $\delta$  149.5, 142.4, 133.8, 117.5, 101.6, 99.2. HRMS for  $\text{C}_6\text{H}_2\text{Br}_2\text{SSe}$  [ $\text{M}^+$ ]: calcd, 343.7409 and 345.7387; found, 343.7408 and 345.7389.

**4,6-Dibromoselenolo[3,4-*b*]selenophene (6Br<sub>2</sub>).** White crystalline solid. 82% yield. M.p.  $69\text{--}70^\circ\text{C}$ .  $^1\text{H}$  NMR (250 MHz,  $\text{CDCl}_3$ )  $\delta$  7.85 (d,  $J = 6$  Hz, 1H), 6.99 (d,  $J = 6$  Hz, 1H).  $^{13}\text{C}$  NMR (62.5 MHz,  $\text{CDCl}_3$ )  $\delta$  151.2, 139.6, 133.2, 121.1, 104.1, 102.2.

**Solid-State Polymerization (SSP).** In a typical experimental procedure, a dibromo compound (one of 3Br<sub>2</sub>–6Br<sub>2</sub>) was placed in a 50 mL round-bottomed flask closed with a stopper. The flask was heated to a temperature that was at least  $5\text{--}10^\circ\text{C}$  below the compound's melting point for a few hours (see Table 1 for details), during which the original white color of the dibromo compound turned black (except 4Br<sub>2</sub>). The appearance of brown bromine vapor in the flask was indicative of the progress of the SSP. After completion of the reaction, the resulting black polymer was collected to afford the bromine-doped polymers. Compounds 3Br<sub>2</sub>, 5Br<sub>2</sub>, and 6Br<sub>2</sub> were polymerized using this SSP method to obtain P3, P5, and P6, respectively. Compound 4Br<sub>2</sub> does not undergo SSP when heated to below its melting point ( $45^\circ\text{C}$ ) for about 1 week. The conductivity of the as-obtained bromine doped polymers was measured in a pressed pellet by the two-probe method.

**Details of Computations.** All calculations were carried out using the Gaussian 03 program.<sup>37</sup> All molecules and polymers were fully optimized without symmetry constraints using a hybrid density functional method,<sup>38</sup> Becke's three-parameter exchange functional combined with the LYP correlation functional (B3LYP)<sup>39</sup> and with the 6-31G(d) basis set (B3LYP/6-31G(d)). The calculations for polymers were performed using Periodic Boundary Conditions (PBC) as implemented in Gaussian 03.<sup>40</sup> The polymer unit cell consists of two monomer units oriented anti to each other. It has been shown that band gaps predicted for conducting polymers using the hybrid B3LYP functional coupled with PBC are in excellent agreement with the experimental values.<sup>28b,41</sup>

(36) Arnanz, A.; Marcos, M.-L.; Delgado, S.; Gonzalez-Velasco, J.; Moreno, C. *J. Organomet. Chem.* **2008**, 693, 3457–3470.


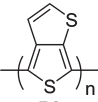

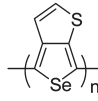

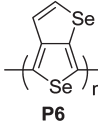
(37) All calculations were performed using the Gaussian 03 program. Frisch, M. J. et al. *Gaussian 03, Revision C.02*; Gaussian, Inc.: Wallingford, CT, 2004. See the Supporting Information for complete citation.

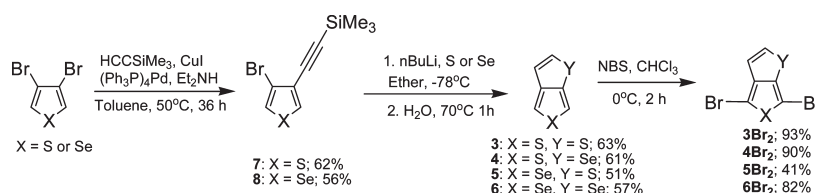
(38) (a) Parr, R. G.; Yang, W. *Density-Functional Theory of Atoms and Molecules*; Oxford University Press: New York, 1989. (b) Koch, W.; Holthausen, M. C. *A Chemist's Guide to Density Functional Theory*; Wiley-VCH: New York, 2000.

(39) (a) Lee, C.; Yang, W.; Parr, R. G. *Phys. Rev. B* **1988**, 37, 785. (b) Becke, A. D. *J. Chem. Phys.* **1993**, 98, 5648.

(40) (a) Kudin, K. N.; Scuseria, G. E. *Chem. Phys. Lett.* **1998**, 289, 611. (b) Kudin, K. N.; Scuseria, G. E. *Phys. Rev. B* **2000**, 61, 16440.

Table 1. Conditions for Solid-State Polymerizations (SSP) and Conductivities for As-Prepared P3, P5, and P6

Monomer	Polymer	Conditions for SSP	Conductivity (S cm <sup>-1</sup> )
 3Br <sub>2</sub>	 P3	50 °C for 2 days	6
 5Br <sub>2</sub>	 P5	45 °C for 4–5 h	0.01
 6Br <sub>2</sub>	 P6	45 °C for 6–8 h	0.22

Scheme 1. Synthesis of Compounds 3–6 and 3Br<sub>2</sub>–6Br<sub>2</sub>

## Results and Discussion

**Synthesis of the Monomers.** The known 3-bromo-4-(trimethylsilyl)ethynylthiophene (**7**) and **3** were synthesized according to the adapted literature procedure<sup>17b,35</sup> from commercially available 3,4-dibromothiophene. The selenium analogue of **7**, 3-bromo-4-(trimethylsilyl)ethynylselenophene (**8**), was obtained by the palladium catalyzed Sonogashira coupling reaction of 3,4-dibromoselenophene with trimethylsilylacetylene in the presence of CuI and diethylamine in toluene at 50 °C. The peripheral<sup>42</sup> heterocyclic ring was constructed by the lithiation of **7** or **8** with 1 equivalent of *n*-BuLi in ether followed by the addition of elemental sulfur or selenium to produce the thiolate or selenolate anion that, after cyclization, gives **3–6** (Scheme 1).

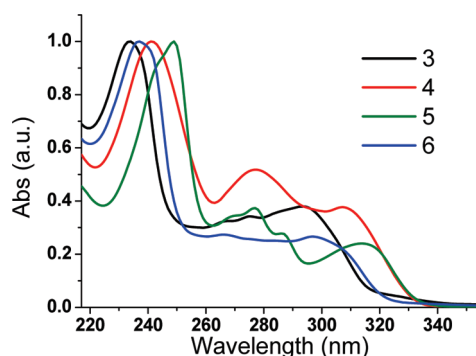
Bromination of **3** with 2 equiv. of NBS in CHCl<sub>3</sub> at 0 °C gives 4,6-dibromothiopheno[3,4-*b*]thiophene (**3Br<sub>2</sub>**) as the sole product with a 93% yield. Two doublets at  $\delta$  7.35 and 6.78 with a coupling constant  $J = 5.6$  Hz corresponding to the 2,3-hydrogens in the peripheral ring supports the interpretation that bromination occurs selectively on the main<sup>42</sup> ring. The structure of **3Br<sub>2</sub>** was also confirmed by X-ray analysis (see below). Bromination of **4** with 2 equivalents of NBS furnished **4Br<sub>2</sub>** with a 90% yield (Scheme 1). Interestingly, bromination of **5** with 2 equiv.

of NBS in CHCl<sub>3</sub> at 0 °C led to the formation of **5Br<sub>2</sub>** with a relatively low yield (41%). Bromination of **5** was performed also at –28 °C; however, the product was again obtained with a relatively low yield. The low yield from the bromination of **5** may be due to partial polymerization of **5Br<sub>2</sub>** during the reaction, and indeed **5Br<sub>2</sub>** polymerizes easily under SSP conditions (see below). Unlike **5**, bromination of **6** with 2 equiv. of NBS gave compound **6Br<sub>2</sub>** with a good yield (82%).

**Absorption Spectroscopy.** The electronic spectra of monomers **3–6** were obtained and compared with the results of DFT calculations. The UV–vis spectra of **3–6** (Figure 1) consist of three absorption peaks. Peaks at around 234–249 nm correspond to the absorption of the main thiophene and selenophene rings, with the selenophene ring absorbing at a longer wavelength than the thiophene ring. We note that parent thiophene absorbs at  $\lambda_{\text{max}} = 232$  nm and parent selenophene absorbs at  $\lambda_{\text{max}} = 249$  nm. Compounds **3–6** have two additional weaker absorption peaks at ~266–277 nm and at ~293–314 nm, which apparently originate from the interaction between the two heterocyclic rings. Again, these peaks are at longer wavelengths for compounds **5** and **6**, which have a selenium atom in the main ring, than for compounds **3** and **4**, which have a sulfur atom in the main ring. The presence of three absorption peaks in the region of 220–320 nm for compounds **3–6** is also nicely reproduced by TD-DFT calculations. The calculated (TD-B3LYP/6-311+G(2df,p)//B3LYP/6-31G(d)) absorption peaks for these compounds (see the Supporting Information; Table S1) are in excellent agreement with the experimental values.

- (41) (a) Pino, R.; Scuseria, G. E. *J. Chem. Phys.* **2004**, *121*, 8113. (b) Cao, H.; Ma, J.; Zhang, G.; Jiang, Y. *Macromolecules* **2005**, *38*, 1123. (c) Kertesz, M.; Choi, C. H.; Yang, S. *Chem. Rev.* **2005**, *105*, 3448.
- (42) Throughout the paper, we refer to the ring that undergoes polymerization (bottom ring in Scheme 1) as the main ring and the ring that does not undergo polymerization (top ring in Scheme 1) as the peripheral or annulated ring.

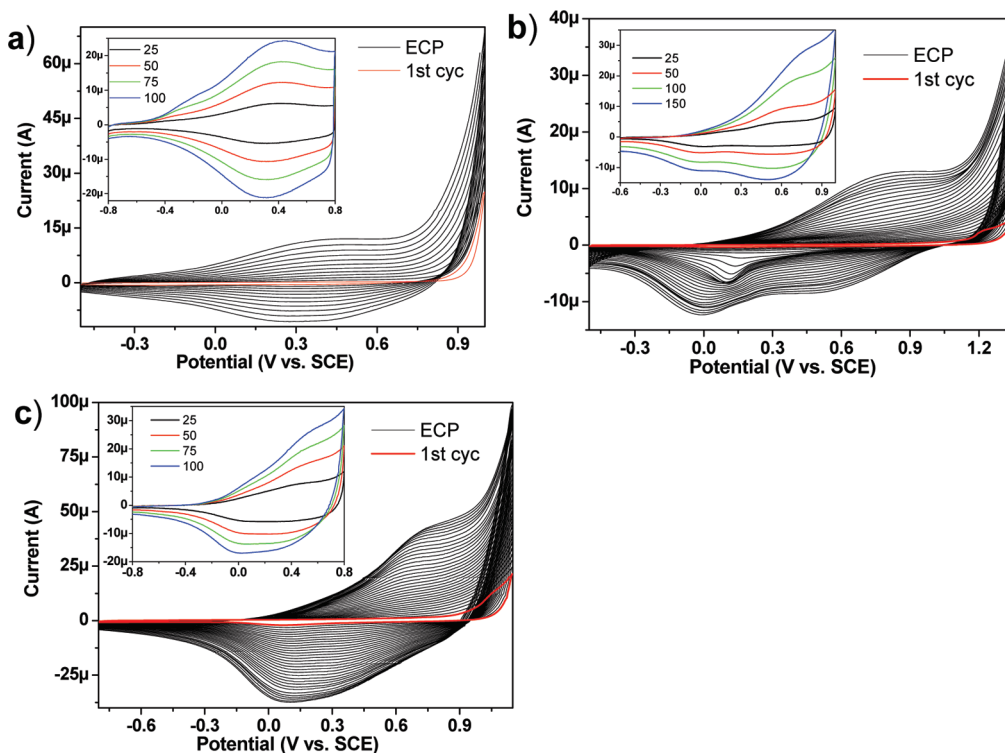
**Electropolymerization.** Monomers **4**, **5**, and **6** were polymerized electrochemically by repetitive cycles over the anodic redox active range of the compounds (Figure 2 for compounds **4–6** and Figure S1 in the Supporting Information for the known<sup>17</sup> electropolymerization of compound **3**). All compounds show an irreversible anodic peak corresponding to the oxidation of the monomers. Electropolymerization of thiophene **4** produces films that are quite stable electrochemically; however, electropolymerization of selenophenes **5** and **6** leads to less electrochemically stable films (electrochemical polymerization of monomer **4** was reported to provide **P4**).<sup>31</sup> For comparison, polyselenophenes of the PEDOS type usually produce films as electrochemically stable as films of PEDOT type polymers.<sup>22,24</sup> The CVs of **P4**, **P5**, and **P6** recorded in a monomer-free electrolytic medium show



**Figure 1.** Normalized UV-vis absorption spectra of monomers **3–6** in acetonitrile.

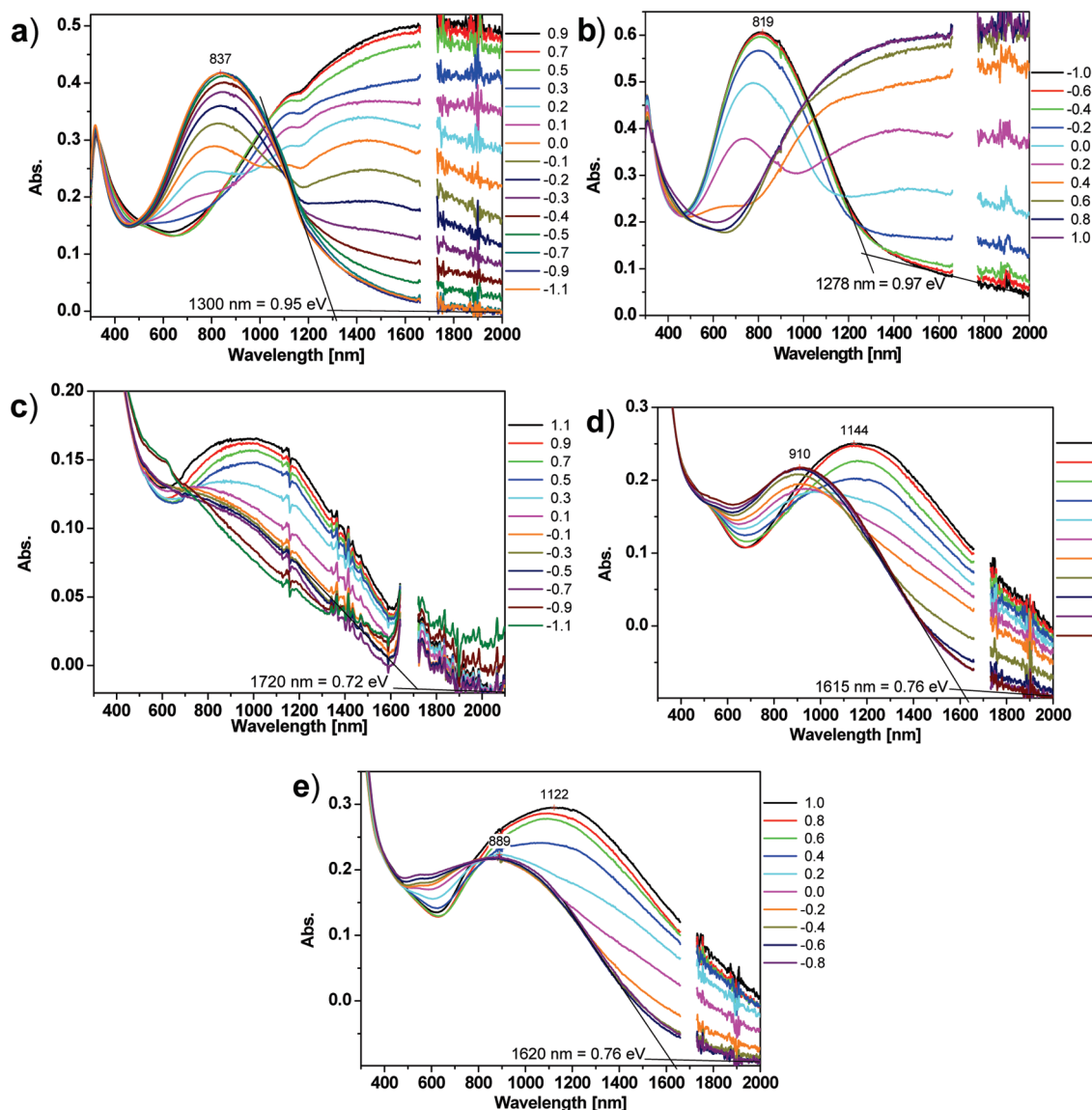
that the polymers are electroactive and stable during first few cycles at different scan rates (insets in Figure 2).

**Spectroelectrochemistry.** Spectroelectrochemical studies of the electrochemically produced polymers, **P4–P6**, were performed to evaluate their electronic properties and band gaps and, consequently, to elucidate the effect of the aromaticity of the annulated heterocyclic ring on the electronic properties of the conjugated polymers. The spectroelectrochemistry of **P4–P6** films obtained on an ITO electrode are shown in Figure 3 (in neutral and p-doped states). For **P4** and **P6**, the measurements (electropolymerization and spectroelectrochemistry) were performed in two different solvents (acetonitrile and PC) and the spectroelectrochemical results are very similar in both solvents (Figure 3a,b,d,e). For **P5**, the measurements were performed in dichloromethane (Figure 3c) because it does not electrodeposit sufficiently in either acetonitrile or PC. The spectroelectrochemically measured optical band gap (extracted from the onset on the  $\pi-\pi^*$  transition) of **P4**, which has a polythiophene backbone and a selenium atom in the peripheral ring, is 0.96 eV ( $\sim 1290$  nm) (Figure 3a,b), which is comparable to the reported optical band gap (0.9 eV).<sup>31</sup> For comparison, the optical band gap of **P3**, in which the heteroatom in the peripheral ring is sulfur, is 0.85 eV.<sup>17a</sup> **P4** is deep-blue in the neutral state and transmissive gray in the p-doped state. Polyselenophene-based **P5**, which has a sulfur heteroatom in the peripheral ring, is predicted to have a very low band gap of about  $\sim 0.6$  eV (after empirical correction of computational results, see computational section below) and the electrodeposited film has an



**Figure 2.** Multisweep electropolymerization of (a) monomer **4** on Pt electrode in TBAPC/acetonitrile; (b) monomer **5** on Pt electrode in TBAPF<sub>6</sub>/dichloromethane; (c) monomer **6** on Pt electrode in TBAPC/acetonitrile. The insets show the CV for the polymers in monomer-free solution at different scan rates between 25 to 150 mV/s.





**Figure 3.** Spectroelectrochemistry of films of (a) **P4** in acetonitrile, (b) **P4** in PC, (c) **P5** in DCM, (d) **P6** in acetonitrile, and (e) **P6** in PC.

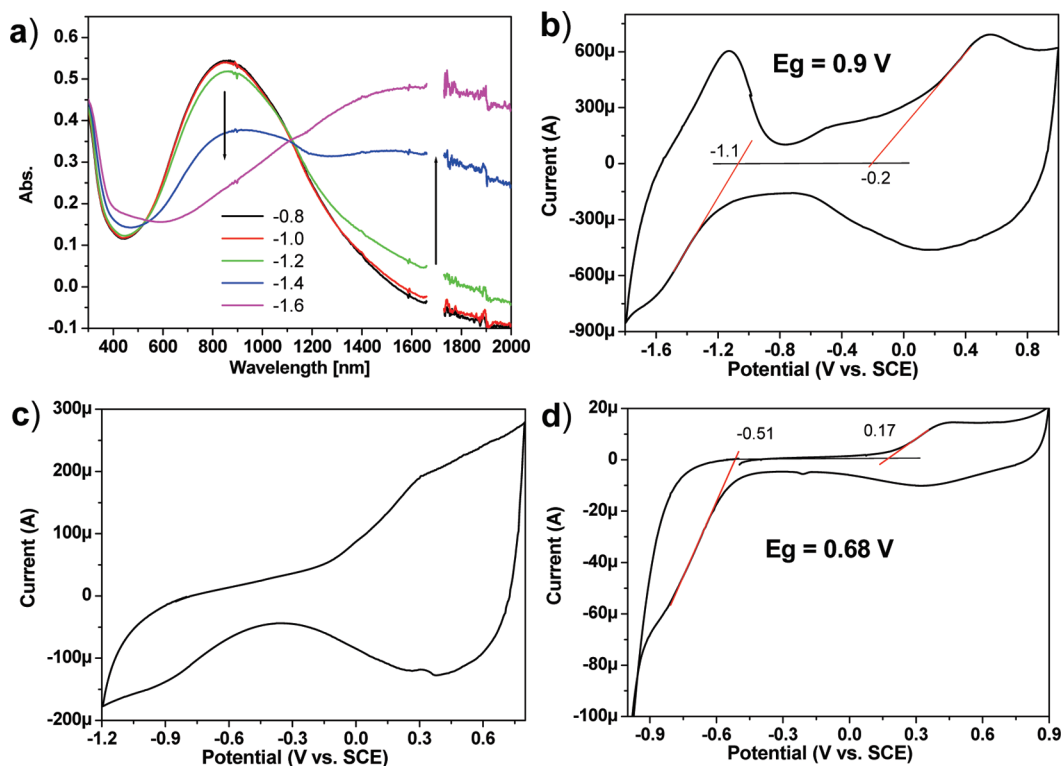
optical band gap is 0.72 eV (Figure 3c). Although optical band gap of **P5** is slightly higher than predicted, **P5** is a very low band gap polymer. The spectroelectrochemistry of polyselenophene-based **P6**, in which the heteroatom in the peripheral ring is selenium, is represented in panels d and e in Figure 3 in acetonitrile and PC, respectively. The absorption peak is estimated to onset at 1620 nm, which corresponds to an optical band gap of 0.76 eV in excellent agreement with calculated values (see below) and makes **P6** a very low band gap polymer. **P5** and **P6** in the electrochemically p-doped state do not have strong absorption in the near IR range, in contrast to their polythiophene analogues, **P3**<sup>17</sup> and **P4**, and to their polyselenophene analogue PEDOS<sup>22</sup> and its derivatives.<sup>24</sup>

Using the optically measured band gap of **P3–P6** we have shown that systematic changes in the band gap can be achieved by replacing the sulfur atom with a selenium atom in the main and peripheral rings,<sup>42</sup> which enables band gap control in this family of low-band-gap conducting polymers. We can summarize that replacing the sulfur atom with a selenium atom in the main heterocyclic ring

(i.e., switching from a polythiophene to a polyselenophene backbone) lowers the band gap; however, replacing the sulfur atom with a selenium atom in the peripheral heterocyclic ring increases the band gap because of the reduced aromatic character of selenophene compared to thiophene (e.g., **P4** and **P6** have higher band gaps than **P3** and **P5**, respectively). The combination of these two trends allows the band gap to be tuned. Importantly, the experimentally obtained band gaps of **P4** and **P6** (measured from the onset of the UV–vis–NIR absorption spectra of the polymers in the neutral state) are in excellent agreement (to within 0.1 eV) with the calculated values (see below).

**N-Type Doping Behavior.** Polythiophenes are known to be more stable under p-type doping than under n-type doping and most polythiophene-based conducting polymers do not show reversible n-type behavior.<sup>43</sup> Spectroelectrochemistry of **P4** under n-type doping is shown in

(43) Holze, R. In *Handbook of Advanced Electronic and Photonic Materials and Devices*; Nalwa, H. S., Ed.; Academic Press: San Diego, CA, 2001; Chapter 6, pp 209–301.



**Figure 4.** (a) Spectroelectrochemistry of **P4** film on ITO showing n-type doping. CV of p- and n-type behavior of (b) **P4**, (c) **P5**, and (d) **P6**.

Figure 4a. **P4** can be fully oxidized at 0.8 V (Figure 3a and 3b) and then reduced stepwise to  $-0.8$  V to the neutral state. Further reduction to  $-1.6$  V resulted in n-type doping that resembled the p-type in terms of absorption with relatively strong absorption in the NIR range. To the best of our knowledge, this is the first spectroelectrochemical study of n-type doping behavior of such type of polymers. Selenophene-based **P5** and **P6** show irreversible n-type behavior and are not as stable under repeated CV cycles in the n-type region.

**Chemical Solid-State Polymerization.** Thiophene-based low-band-gap conductive polymers are well studied and their electropolymerization was frequently reported.<sup>2,9</sup> However, limited number of reports on chemical polymerizations leading to low-band-gap conductive polymers have appeared. Pomerantz et al., reported<sup>16</sup> the chemical polymerization of **P2** with 1 equiv. of  $\text{FeCl}_3$  to produce a soluble polymer, whereas polymerization with 4 equiv. of  $\text{FeCl}_3$  produces an insoluble polymer with a relatively low conductivity of  $7.2 \times 10^{-2} \text{ S cm}^{-1}$  and band gap of 0.92–0.98 eV. More recently, it was reported that chemical polymerization of **3** with  $\text{FeCl}_3$  produces conductive **P3** (conductivity of  $2 \text{ S cm}^{-1}$ ) in the oxidized state.<sup>18b</sup> Oxidative chemical polymerizations of monomers **3–6** are expected to produce defects in the polymer chains because of the possibility for branching through the peripheral ring, which may lead to two-dimensional propagation of the

polymer chains and decrease the conjugation. To obtain highly conjugated and well-ordered conductive polymers and avoid cross-linkages, we used a recently developed solid-state polymerization (SSP)<sup>44,45</sup> method that requires mild polymerization conditions and is especially useful for the preparation<sup>22</sup> of polyselenophenes because of their lower polymerization temperature (Scheme 2).

Compound **3Br<sub>2</sub>** was polymerized via SSP under slight heating ( $50^\circ\text{C}$ ) for 2 days (Table 1). The resulting bromine-doped black polythiophene **P3** is completely insoluble in common organic solvents and as-obtained **P3** has a relatively high conductivity of  $\sim 6 \text{ S cm}^{-1}$  (measured in a pressed pellet by the two probe method).<sup>46,47</sup> The conductivity value is similar to that of similarly prepared PEDOT and PEDOS measured by the same method and it is even slightly higher than the previously reported conductivity of chemically polymerized **P3** ( $2 \text{ S cm}^{-1}$ ).<sup>18b</sup> Our attempt to use SSP for the preparation of **P4** failed because of the low melting point of **4Br<sub>2</sub>** ( $52^\circ\text{C}$ ). Selenophene-based dibromo-compounds **5Br<sub>2</sub>** and **6Br<sub>2</sub>** undergo SSP more easily than thiophene-based dibromo-compound **3Br<sub>2</sub>**. Compounds **5Br<sub>2</sub>** and **6Br<sub>2</sub>** were successfully polymerized using the solid-state method by slight heating at  $45^\circ\text{C}$  for 4–8 h to obtain black polymers **P5** and **P6**, respectively (Table 1). The resulting bromine-doped polymers are also completely insoluble in common organic solvents.<sup>48</sup> However, **P5** and **P6** have

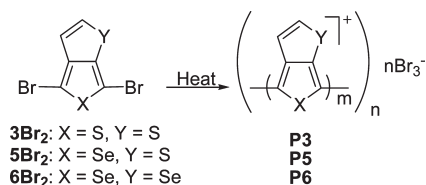
(44) (a) Meng, H.; Perepichka, D. F.; Wudl, F. *Angew. Chem., Int. Ed.* **2003**, *42*, 658–661. (b) Meng, H.; Perepichka, D. F.; Bendikov, M.; Wudl, F.; Pan, G. Z.; Yu, W.; Dong, W.; Brown, S. *J. Am. Chem. Soc.* **2003**, *125*, 15151–15162. (c) Spencer, H. J.; Berridge, R.; Crouch, D. J.; Wright, S. P.; Giles, M.; McCulloch, I.; Coles, S. J.; Hursthouse, M. B.; Skabara, P. J. *J. Mater. Chem.* **2003**, *13*, 2075–2077.

(45) Lepeltier, M.; Hiltz, J.; Lockwood, T.; Bélanger-Gariépy, F.; Perepichka, D. F. *J. Mater. Chem.* **2009**, *19*, 5167–5174.

(46) Wudl, F.; Bryce, M. R. *J. Chem. Educ.* **1990**, *67*, 717–718.

(47) We note that actual conductivity might be significantly higher because of relatively large contact resistance for materials with high conductivity in the two-probe method. See also ref 45.



Scheme 2. Solid-State Polymerization of **3Br<sub>2</sub>**, **5Br<sub>2</sub>**, and **6Br<sub>2</sub>**

relatively low conductivities of  $\sim 0.01$  and  $0.22 \text{ S cm}^{-1}$ , respectively, in the doped state (measured in a pressed pellet by the two-probe method)<sup>46</sup> in contrast to **P3**, which has a relatively high conductivity (Table 1).

**X-ray Analysis.** Only a few crystal structures of thienofused thiophene derivatives have been reported in the literature,<sup>49</sup> and no crystal structure of thieno[3,4-*b*]thiophene (**3**) or of any selenolo fused thiophene derivatives are known. Single crystals of thiophene-based **3Br<sub>2</sub>** and **4Br<sub>2</sub>** were grown from a mixture of chloroform and hexane ( $\sim 5\%$ ) by slow evaporation at low temperature ( $\sim 4^\circ\text{C}$ ). The unit cell of **3Br<sub>2</sub>** crystals comprises two independent molecules. The peripheral<sup>42</sup> ring of one of the molecules has a disordered structure (Figure 5). For discussion, we use the geometry of the other independent molecule, which is not disordered. The unit cell of **4Br<sub>2</sub>** crystals also comprises two independent molecules, both having disordered structures (Figure 6). The average bond lengths in two independent molecules are used for the discussion of **4Br<sub>2</sub>**. Both **3Br<sub>2</sub>** and **4Br<sub>2</sub>** are planar and their crystals exhibit two types of packing:  $\pi$ - $\pi$  stacking and a herringbone pattern (see Figures S2 and S3 in the Supporting Information). All C-C bond lengths in **3Br<sub>2</sub>** are very similar (within  $0.01 \text{ \AA}$ ) to those in **4Br<sub>2</sub>**, which is in agreement with the calculated (B3LYP/6-31G(d)) geometries of **3Br<sub>2</sub>** and **4Br<sub>2</sub>** (see Table S3 in the Supporting Information). In **3Br<sub>2</sub>**, the bond lengths and angles in the main thiophene ring<sup>42</sup> are similar to those of many other previously reported thiophene derivatives, whereas the annulated<sup>42</sup> thiophene ring has somewhat different bond lengths, consistent with the presence of two exocyclic double bonds. X-ray analysis of **3Br<sub>2</sub>** reveals its shortest intermolecular Br $\cdots$ Br, Br $\cdots$ S, and S $\cdots$ S distances to be  $3.60$ ,  $3.56$ , and  $3.58 \text{ \AA}$ , respectively (see Figure S2 in the Supporting Information). X-ray analysis of **4Br<sub>2</sub>** reveals its shortest intermolecular Br $\cdots$ Br, Br $\cdots$ S, Br $\cdots$ Se, S $\cdots$ S, and Se $\cdots$ Se distances to be  $3.49$ ,  $3.41$ ,  $5.24$ ,  $3.49$ , and  $3.62 \text{ \AA}$ , respectively (see Figure S3 in the Supporting Information), which are within the van der Waals radii of Br ( $1.85 \text{ \AA}$ ) and S ( $1.80 \text{ \AA}$ ) and somewhat shorter than

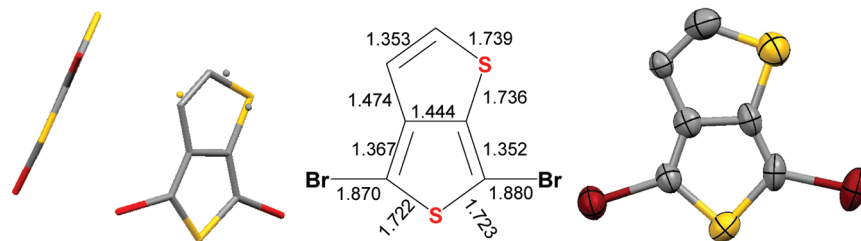
similar distances in **3Br<sub>2</sub>**. For comparison, the shortest intermolecular Br $\cdots$ Br distance in 2,5-dibromo-3,4-ethylenedioxythiophene (DBEDOT) is  $3.45 \text{ \AA}$ .<sup>44b</sup> It could be suggested that the short intermolecular Br $\cdots$ Br distances are responsible for the observed solid-state polymerization of **3Br<sub>2</sub>**; however, **4Br<sub>2</sub>** has even shorter intermolecular Br $\cdots$ Br distances and does not undergo SSP (although the melting point of **4Br<sub>2</sub>** is  $7^\circ\text{C}$  lower than that of **3Br<sub>2</sub>**, which prevents direct comparison). Indeed, recent work on SSP concluded that “the intermolecular Hal/Hal contacts, which were suggested earlier to be important, do not appear to be critical for the solid-state polymerization”,<sup>45</sup> which is in line with our observations. The interplane distance between  $\pi$ - $\pi$ -stacked molecules in **3Br<sub>2</sub>** is  $3.49 \text{ \AA}$ , which is practically the same as in DBEDOT<sup>44b</sup> ( $3.50 \text{ \AA}$ ), whereas the interplane distance between  $\pi$ - $\pi$ -stacked molecules in **4Br<sub>2</sub>** is slightly larger ( $3.57 \text{ \AA}$ ) because of the larger size of the selenium atom (the interplane distance between  $\pi$ - $\pi$ -stacked molecules in 2,5-dibromo-3,4-ethylenedioxysephenene (DBEDOS)<sup>22</sup> is  $3.64 \text{ \AA}$ ).

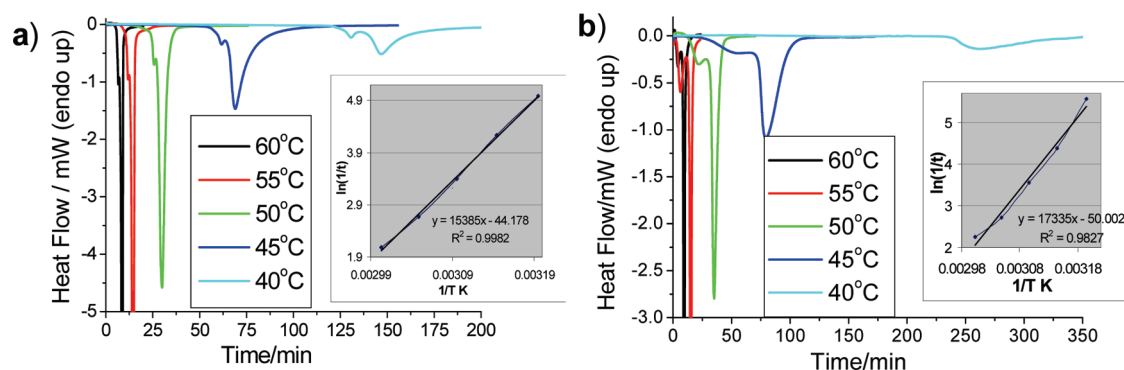
**Differential Scanning Calorimetric (DSC) Studies of Solid-State Polymerization (SSP).** We used DSC to follow the SSP process of **3Br<sub>2</sub>**–**6Br<sub>2</sub>**. Heating the dibromo compounds **3Br<sub>2</sub>**–**6Br<sub>2</sub>** at a scan rate of  $10^\circ\text{C/min}$  results first in endothermic melting followed by exothermic polymerizations of the melted samples (Figure 7). The melting of compounds **3Br<sub>2</sub>**–**6Br<sub>2</sub>** requires  $4.0$ ,  $3.7$ ,  $4.0$ , and  $5.0 \text{ kcal/mol}$ , respectively. Selenophene-based dibromo compounds **5Br<sub>2</sub>** and **6Br<sub>2</sub>** show sharp exothermic polymerization peaks at significantly lower temperatures than their thiophene-based analogues **3Br<sub>2</sub>** and **4Br<sub>2</sub>** (Figure 7).

The kinetics of the SSP of **5Br<sub>2</sub>** and **6Br<sub>2</sub>** was studied by isothermal DSC measurements at  $40$ – $60^\circ\text{C}$  (below their melting points) (Figure 8). Extrapolation of the Arrhenius plot<sup>50</sup> to  $20^\circ\text{C}$  predicts the half lifetime of compound **5Br<sub>2</sub>** to be  $\sim 2.5$  days, which is in good agreement with our observation of SSP of **5Br<sub>2</sub>** at room temperature. By comparison, similar extrapolations to  $20^\circ\text{C}$  predict half lifetimes of about 20 days for DBEDOS<sup>22</sup> and of about 70 days for DBEDOT.<sup>44b</sup> A comparison of the SSP data from the DSC measurements indicates that compound **5Br<sub>2</sub>** polymerizes at a temperature that is  $\sim 20^\circ\text{C}$  lower than the polymerization temperature of DBEDOS and  $\sim 40^\circ\text{C}$  lower than that of DBEDOT. The DSC-measured activation energies for the SSP of **5Br<sub>2</sub>** ( $30.5 \text{ kcal/mol}$ ) and **6Br<sub>2</sub>** ( $34.7 \text{ kcal/mol}$ )<sup>51</sup> are higher than for DBEDOS ( $27.5 \text{ kcal/mol}$ )<sup>22</sup> and DBEDOT<sup>44b</sup> ( $27.1 \text{ kcal/mol}$ ). However, the half lifetimes of **5Br<sub>2</sub>** and **6Br<sub>2</sub>** are shorter than those of DBEDOT and DBEDOS because of their higher activation entropies.

- (48) The possibility of significant direct bromination by released molecular bromine of the polymer produced by SSP can be excluded based on IR spectrum of the produced polymer (see Figure S4 in the Supporting Information). The calculated (B3LYP/6-31G(d)) C–Br vibration stretch (strong peak) in brominated compound **5** is predicted at  $868$  or  $916 \text{ cm}^{-1}$  (depending on isomer; frequencies are unscaled). However, there is no peak around  $900 \text{ cm}^{-1}$  in the IR spectrum of bromine-doped **P5**.
- (49) (a) Amaresh, R. R.; Lakshmikantham, M. V.; Baldwin, J. W.; Cava, M. P.; Metzger, R. M.; Rogers, R. D. *J. Org. Chem.* **2002**, *67*, 2453–2458. (b) Matsumura, N.; Tanaka, H.; Yagyu, Y.; Mizuno, K.; Inoue, H.; Takada, K.; Yasui, M.; Iwasaki, F. *J. Org. Chem.* **1998**, *63*, 163–168. (c) Yoneda, S.; Ozaki, K.; Inoue, T.; Sugimoto, A.; Yanagi, K.; Minobe, M. *J. Am. Chem. Soc.* **1985**, *107*, 5801–5802.

- (50) For the Arrhenius plots, we used the maximum reaction rate (peak maximum at DSC curves) as a substitute for  $t_{1/2}$ , following ref 44b. We note that while there is no solid theoretical support for the validity of such Arrhenius plots it was successfully applied earlier<sup>22,44b</sup> and gives very reasonable estimation of half lifetimes. In each experiment, the same amount of compound from the same batch was used to eliminate the effect of impurities, crystallite size, etc.
- (51) We note that Arrhenius plot (Figure 8b) of SSP of **6Br<sub>2</sub>** is deviating from linearity.



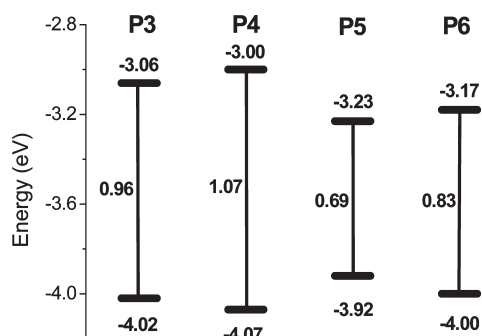


**Figure 8.** Isothermal DSC curves and (insets) Arrhenius plots for the solid-state polymerization at different temperatures of compounds (a) **5Br<sub>2</sub>** and (b) **6Br<sub>2</sub>**.

**Table 2.** Calculated Bond Lengths, HOCO (Highest Occupied Crystal Orbital) and LUCO (Lowest Unoccupied Crystal Orbital) Energies (at B3LYP/6-31G(d)), and Experimental Optical Band Gaps for P3–P6

polymers	fused (Å) <sup>a</sup>	inter-ring (Å) <sup>b</sup>	HOCO (eV)	LUCO (eV)	band gap (eV)	
					calcd <sup>c</sup>	expt <sup>d</sup>
<b>P3</b>	1.424	1.424	−4.02	−3.06	0.96	0.85 <sup>17b</sup>
<b>P4</b>	1.428	1.426	−4.07	−3.00	1.07	0.96
<b>P5</b>	1.427	1.412	−3.92	−3.23	0.69	0.72
<b>P6</b>	1.429	1.415	−4.00	−3.17	0.83	0.76

<sup>a</sup> Fused C–C bond length. <sup>b</sup> Inter-ring C–C bond length. <sup>c</sup> Calculated band gap. <sup>d</sup> Experimental optical band gap obtained from spectroelectrochemical data.



**Figure 9.** Comparison of the calculated energy levels of **P3–P6** at B3LYP/6-31G(d).

achievement of band gap control in very low band gap (< 1.0 eV) conjugated polymers.

### Conclusions

The paper reports new strategy for the band gap control in very low band gap (< 1.0 eV) polymers. A series of new low-band-gap conjugated polyselenophenes and polythiophenes was systematically prepared by electropolymerization (**P4**, **P5**, and **P6**) and by solid-state polymerization (**P3**, **P5**, and **P6**). We have also presented the synthesis of monomers **4**, **5**, and **6**, followed by their bromination. The first X-ray structures of thieno[3,4-*b*]thiophene and selenolo[2,3-*c*]thiophene derivatives, i.e., of **3Br<sub>2</sub>** and **4Br<sub>2</sub>**, are also presented. Electropolymerization of **4**, **5**, and **6** affords **P4**, **P5**, and **P6**, respectively, and

the spectroelectrochemically measured band gaps of these polymers are 0.96, 0.72, and 0.76 eV, respectively. DFT calculations performed on **P3–P6** provide excellent estimations of the band gaps of the corresponding polymers.

We introduced a new scheme for band gap control in conjugated polymers by replacing the sulfur atom with a selenium atom in the main and/or peripheral ring,<sup>42</sup> which leads to significant and predictable changes in the band gap of the polymers. This is due to the different aromaticities of thiophene and selenophene rings, with the selenophene ring being less aromatic than the thiophene ring. The use of different combinations of selenium and sulfur atoms in the main and peripheral rings<sup>42</sup> leads, for the first time, to the achievement of band gap control in very low band gap (< 1.0 eV) conjugated polymers.

**Acknowledgment.** We thank the Israel Science Foundation, the Estate of George Talis Foundation, and the Helen and Martin Kimmel Center for Molecular Design for financial support. M.B. is the incumbent of the Recanati career development chair, a member ad personam of the Lise Meitner-Minerva Center for Computational Quantum Chemistry, and acknowledges DuPont for a Young Professor Award.

**Supporting Information Available:** CIF files; electrochemical data for compound **3**, details of calculations, and complete citation of reference 37 (PDF). This material is available free of charge via the Internet at <http://pubs.acs.org>.